ACS APPLIED MATERIALS & INTERFACES

Research Article

www.acsami.org

Photopolymerized Network Polysiloxane Films with Dangling Hydrophilic/Hydrophobic Chains for the Biofouling Release of Invasive Marine Serpulid *Ficopomatus enigmaticus*

Elisa Martinelli,[†] Ilaria Del Moro,[†] Giancarlo Galli,*[,†] Martina Barbaglia,[‡] Carlo Bibbiani,[‡] Elvira Mennillo,[‡] Matteo Oliva,[‡] Carlo Pretti,[‡] Diego Antonioli,[§] and Michele Laus[§]

[†]Dipartimento di Chimica e Chimica Industriale and UdR Pisa INSTM, Università di Pisa, 56124 Pisa, Italy

[‡]Dipartimento di Scienze Veterinarie, Università di Pisa, 56126 Pisa, Italy

[§]Dipartimento di Scienze ed Innovazione Tecnologica, Università del Piemonte Orientale, 15100 Alessandria, Italy

Supporting Information

ABSTRACT: Novel photopolymerized network films based on a polysiloxane matrix containing varied amounts of polyoxyethylene (P3) or perfluorohexylethyl (F) dangling side chains were investigated. For films containing less than 10 wt % P3 and F, the wettability and elastic modulus were similar to those of the photopolymerized network matrix. However, angle-resolved X-ray photoelectron spectroscopy measurements proved that the surface of films with F dangling chains was highly enriched in fluorine depending on both the amount of P3 and F and their relative ratio in the films. The biological performance of the films was evaluated against a new widespread and invasive marine biofoulant, the serpulid *Ficopomatus enigmaticus*. The diatom *Navicula salinicola* was also assayed as a conventional model organism for comparison. Films richer in P3 better resisted the settlement and promoted the release of calcified tubeworms of *F. enigmaticus*.

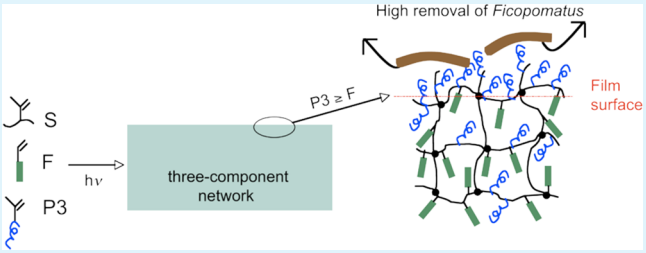

KEYWORDS: *amphiphilic polymer, photopolymerized network, marine biofouling, fouling-release film, Ficopomatus enigmaticus, Navicula salinicola*

1. INTRODUCTION

Understanding the correlation between the structure and the properties of the surface of a material may lead to novel developments in a number of fields where interfacial interactions, operating within a few nanometers of a surface, are critical. Biofouling is an example of a nanoscale adhesion process, occurring at the interface between fouling organisms and all the man-made surfaces, in both marine and freshwater environments. Nowadays, biocide-containing antifouling coatings are effective in combating marine biofouling, but their use is becoming more restricted because of issues of toxicity to and accumulation/persistence in the aquatic environment.[1−4] Accordingly, in recent years, a more environmentally friendly approach is being pursued by replacing traditional biocidal coatings with antifouling (AF) coatings that prevent the settlement (attachment) of the colonizing fouling organisms or fouling-release (FR) coatings that reduce the adhesion of organisms so that they are removed by hydrodynamic forces such as those generated as a ship moves through the water.[5] Recently, amphiphilic polymers have arisen as attractive candidates for use in FR coatings,[6] as their film surfaces are suggested to have local nanoscale heterogeneities that deter the settlement of organisms and also minimize the intermolecular interactions between biomolecules and substratum. One common strategy to create amphiphilic surfaces is to combine poly(ethylene glycol)s with fluoropolymers. Such examples include hyperbranched fluoropolymer-poly(ethylene glycol) cross-linked systems,[7,8] copolymers with grafted ethoxylated-fluoroalkyl side chains dispersed in poly(styrene-b-(ethylene-co-butylene)-b-styrene) (SEBS) or poly(dimethylsiloxane) (PDMS) matrices,[9−12] polyurethane coatings prepared from poly(dimethylsiloxane) macromers,[13] and photocured coatings consisting of perfluoropolyether and poly(ethylene glycol).[14,15]

Following this last approach, an easy and versatile method to prepare novel amphiphilic network films is described here based on the UV photo-cross-linking copolymerization of commercially available poly(dimethylsiloxane) (S), polyoxyethylene (P3), and perfluoroalkyl (F) (meth)acrylate (macro)monomers (Figure 1). The choice of a polyfunctional PDMS-like precursor S as a main building block for constructing the elastomeric matrix of the amphiphilic networks was inspired by the fact that PDMS-based films were proven to be very effective FR coatings in laboratory and field trial tests, for example, compared to commercial Intersleek 700 coating.[16] On the other

Received: February 16, 2015
Accepted: April 2, 2015
Published: April 2, 2015

DOI: 10.1021/acsami.5b01522
ACS Appl. Mater. Interfaces 2015, 7, 8293−8301

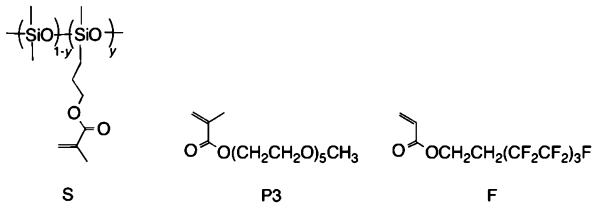

Figure 1. Molecular structures of the macromonomer and monomers used for the matrix (S) and the dangling chains (P3 and F), respectively.

hand, perfluoroalkyl F and polyoxyethylene P3 building blocks with one-functionalized chain end were introduced as dangling side chains to allow for flexibility and mobility,[14] thus favoring their migration to or otherwise away from the film surface when in contact with different external environments.

PDMS-based materials used for marine coatings are generally produced by condensation and hydrosilylation cross-linking reactions.[5] However, the replacement of those processes by a photo-cross-linking process to afford novel marine AF/FR coatings might bring several advantages including (i) avoiding the use of heavy metal-based (e.g., tin-based) catalysts, (ii) reduction in solvent consumption and the associated prolonged periods of time for drying, and (iii) shorter reaction times at room temperature without heating for the finishing step. Only a few examples are reported on curing polysiloxanes by photochemical reactions, for example, in ref 17.

Much attention has been paid to the AF/FR effectiveness of polymer coatings with a variety of microfoulants and macrofoulants, most common test organisms being bacteria, algae, and barnacles at different stages of their life cycles.[18−21] However, essentially nothing is known of the AF/FR properties of coatings against the serpulid *Ficopomatus enigmaticus*,[22] a reef builder tubeworm widespread in Northern and Southern hemispheres.[23−25] It is widely represented in the Mediterranean Sea and is especially invasive among the biofouling community in colonizing submerged surfaces. Recently, Gabilondo et al.[26] published results about the life cycle, the spawning of gametes and fertilization, and the production of competent larvae ready to settle on model surfaces such as PDMS, polystyrene, and glass.

In this work, the biological performance of photopolymerized network films was investigated with *F. enigmaticus* by quantifying the number of larvae or tube-formed worms that settled (attached) on the surfaces within a defined period of time and the adhesion strength of tube-formed worms under a calibrated shear stress. The results are also discussed with respect to the FR properties shown by the same surfaces against the diatom *Navicula salinicola*, taken as a commonly accepted model organism.

2. EXPERIMENTAL SECTION

2.1. Materials. (3-Methacryloxypropyl)trimethoxysilane (MAPTS) (ABCR) and 2-hydroxy-2-methyl propiophenone (HMPP) (Aldrich) were used without further purification. (Methacryloxypropyl)-methylsiloxane−dimethylsiloxane copolymer with 2−4 mol % methacrylate groups (S) (y = 0.02−0.04, M_n = 15 400 g mol^{-1}, M_w/M_n = 3.2) (ABCR), 1*H*,1*H*,2*H*,2*H*-perfluorooctyl acrylate (F) (Fluoryx), and polyethylene glycol monomethyl ether methacrylate (P3) (M_n = 300 g mol^{-1}, M_w/M_n = 1.2) (Aldrich) were dissolved in dichloromethane and passed through a basic alumina chromatographic column (1 cm × 3 cm) to remove the inhibitor.

2.2. Preparation of Glass Substrates. Glass microscope slides (76 × 26 mm^2) were cleaned in piranha solution (concentrated sulfuric acid + 30 wt % hydrogen peroxide, 7/3 v/v) at 80 °C for 1 h and then rinsed with distilled water and acetone and dried in the oven at 100 °C for 10 min. The slides were soaked in a 1% (wt/v) solution of MAPTS in ethanol overnight. Nonreacted MAPTS was washed away with ethanol, and then the residual solvent was removed in the oven at 120 °C for 30 min.

2.3. Preparation of Cross-Linked Films. Fluorinated acrylate F or polyoxyethylene methacrylate P3 were alternatively or simultaneously added to the polyfunctional polysiloxane macromonomer S to prepare two- or three-component mixtures, respectively. In any case, 1 wt % photoinitiator HMPP was first dissolved in S, and subsequently F or P3 was added in the selected amounts (see below). Since P3 is not miscible with S or F, ethyl acetate (∼20 wt %) was added as a cosolvent to get homogeneous and clear mixtures.

The polymer films were photo-cross-linked with a 400 W high pressure Hg lamp (Polymer 400, Helios Italquartz) with energies of 11 000 and 12 400 mW cm^{-2} at 254 and 365 nm, respectively, at an approximately 15 cm distance from the sample. Photo-cross-linking runs were carried out at different UV irradiation times (10−40 min) to identify the optimal reaction conditions. Films for dynamic-mechanical analyses were prepared by curing mixtures in a Teflon mold by UV irradiation for 30 min (final thickness ∼1 mm). Films for all other characterizations were prepared by casting the mixtures on 76 × 26 mm^2 MAPTS-functionalized glass slides and then curing by exposure to UV radiation for 30 min (final thickness ∼400 μm).

Films derived from two-component mixtures are indicated as S*x*P3 and S*x*F, where x is the wt % of S in the mixture. Films derived from three-component mixtures are indicated as S*x*P3F*m*/*n*, where x and m/n are the weight percentage of S in the mixture and the P3/F weight ratio in the remaining portion (100 − x), respectively, that is, 70/30 (7/3), 50/50 (5/5), and 30/70 (3/7). Films, named S100, not containing either the F or the P3 monomer, were also prepared as reference samples.

2.4. Characterization. Infrared spectra were recorded with a Spectrum One PerkinElmer Fourier-transform infrared spectrophotometer with 4 cm^{-1} resolution. Polymer films were cast on a KBr crystal plate (thickness ∼30 μm).

Differential scanning calorimetry (DSC) measurements were performed with a Mettler DSC 30 instrument. Samples of 15−25 mg were used with 10 °C min^{-1} heating/cooling rate. Temperature and energy were calibrated with standard samples of tin, indium, and zinc. The glass transition temperature (T_g) was taken as the inflection temperature in the second heating cycle.

Dynamic-mechanical thermal analyses (DMTA) were carried out by using a Rheometric DMTA V analyzer, employing the single cantilever flexural geometry. The analysis was performed in the linear viscoelasticity regime at the frequency of 1 Hz with a scanning rate of 4 °C min^{-1} in the range −140−150 °C on specimens machined into bars with size of 20 × 5 × 1 mm^3. The storage modulus (E'), loss modulus (E''), and loss factor (tan $\delta = E''/E'$) were determined. Each measurement was performed at least three times on different bar specimens of the same sample.

Contact angles were measured by the sessile drop method with a FTA200 Camtel goniometer using water (θ_w) (J.T. Baker), isopropanol (θ_{ip}) (Aldrich), and *n*-hexadecane (θ_h) (Aldrich) of the highest purity available as wetting liquids. The measured values of θ_w and θ_h were then used to extract the surface tension (γ_S) of the polymer films by the so-called Owens−Wendt−Kaelble method.[27,28]

Angle-resolved X-ray photoelectron spectroscopy (XPS) spectra were recorded by using a PerkinElmer PHI 560 spectrometer with a standard Al−Kα source (1486.6 eV) operating at 350 W. The working pressure was less than 10^{-8} Pa. Extended (survey) spectra were collected in the range of 0−1350 eV (187.85 eV pass energy, 0.4 eV step, 0.05 s step^{-1}). Detailed spectra were recorded for the following regions: Si (2p), C (1s), O (1s), and F (1s) (11.75 eV pass energy, 0.1 eV step, 0.1 eV s step^{-1}). The spectra were recorded at the two photoemission angles ϕ (between the surface normal and the path taken by the photoelectrons) of 70° and 20°, corresponding to

DOI: 10.1021/acsami.5b01522
ACS Appl. Mater. Interfaces 2015, 7, 8293−8301

sampling depths of ∼3 nm and ∼10 nm, respectively. The atomic percentage, after a Shirley-type background subtraction,[29] was evaluated using the PHI sensitivity factors (±1% experimental error). To take into account charging problems, the C (1s) peak was considered at 285.0 eV, and the peak BE differences were evaluated.

2.5. Water Swelling Tests. The films coated on glass slides were soaked in deionized water for different periods of time (t = 0, 24, 48, 72 h) up to 20 days (t = 480 h). The weight percentage of swelling degree was determined by the equation

$$wt\%_{\text{swelling}} = 100 \times (W_{\text{wet}} - W_{\text{dry}})/W_{\text{dry}} \quad (1)$$

where W_{wet} and W_{dry} are the weights of the wet and dry films, respectively.

2.6. Ecotoxicological Tests. Ecotoxicological assays were performed on the film leachates using *Vibrio fischeri*, *Dunaliella tertiolecta*, and *Artemia salina* as test organisms according to a previous procedure[30] (see Supporting Information).

2.7. Biological Assays with *F. enigmaticus*. AF/FR efficacy was assessed on selected surfaces in a settlement/detachment assay with the serpulid polychaete *F. enigmaticus*. Briefly, the settlement of the serpulids to sample surfaces was evaluated with two different methods together with the evaluation of their removal rate under a calibrated wall shear stress in a turbulent channel flow apparatus (TCFA).

2.7.1. Turbulent Channel Flow Apparatus. The TCFA was built as proposed by Schultz et al.[36] with slight modifications. A 500 L reservoir tank was filled with marine water (19 ± 1 °C; salinity 30‰); water flow was generated by the use of an immersion pump that was connected with the entire apparatus. An ultrasound flow meter (Ultrasonic Flow Transmitter DW-S) (accuracy ±2%) was used to evaluate the flow rate. The channel was made in Plexiglas, with a 7.2 × 10.4 mm^2 rectangular section; the total length was 1050 mm. A columnar differential piezometer allowed pressure difference measurement between two out of four different points along the channel apparatus. Following eq 2,[31] it was possible to obtain shear stress value on the wall:

$$\tau_w = -H/2\mathrm{d}P/\mathrm{d}x \quad (2)$$

where τ_w is the shear stress value, H is the section height, and $\mathrm{d}P/\mathrm{d}x$ is the pressure gradient. The instrument was calibrated by measurement of flow rate and pressure gradient along the channel (see Supporting Information). The removal assay was carried out at the maximum shear stress of 28 Pa (Reynolds number Re > 26 000).

2.7.2. F. enigmaticus (Gamete Emission, Fertilization, and Larvae). A *F. enigmaticus* adult colony was collected in Viareggio's harbor (Italy). The colony was taken to the laboratory by using polypropylene jars and maintained in 30 L aquarium for at least 48 h under aeration (20 ± 1 °C, salinity 30‰, pH 8.12). After 48 h, *F. enigmaticus* gametes were collected using a destructive method.[26,31−33] Briefly, calcareous tubes were gently broken, and single worms were rinsed and put in a 0.5 mL drop of filtered natural seawater (FNSW). Gametes were generally released within 10−15 min. Sperm and eggs from 32 females and eight males were collected by pipetting. Male and female gametes were then put together in 50 mL of FNSW for fertilization (20 ± 1 °C). After 1 h, the gamete suspension was filtered twice: first through a 300 μm nylon mesh to remove calcareous debris and adult parts, successively through a 30 μm nylon mesh to collect fertilized eggs by removing unfertilized ones and sperm excess. Fertilized eggs were then resuspended in 2 L of FNSW with a water renewal every 2 days; after each renewal, water was inoculated with a 5 × 10^4 cells mL^{-1} algal suspension of *Isochrysis galbana* for larval feeding. Four days after fertilization, ∼4000 living metatrochophores were obtained. Total number of metatrochophores was estimated by 20 counts of 0.5 mL of FNSW with suspended larvae.

Observations about morphology and time of development of trochophores/metatrochophores were consistent with previous findings.[26] Competent larvae were obtained within 5−6 days from fertilization.

2.7.3. Settlement of F. enigmaticus ("Choice" Experiment). The method consisted in a resuspension of larvae (collected by filtration, 30 μm mesh size) in three different square section polypropylene boxes filled with 1 L of fresh FNSW (∼1000 larvae per beaker) and an algal suspension as stated before. Since the presence of biofilm on surfaces was reported to be a predisposing factor for the adhesion of competent larvae of serpulids,[26,34,35] glass and coated sample slides (six replicates) were exposed for 10 days to a natural biofilm in a recirculating 200 L aquarium system before the test was started. Subsequently, all slides were randomly divided in each box (16 slides per box) and left submerged in vertical position for 18 days until a 2−4 mm secondary calcified tube was visible; only calcified tube-formed worms adhered on the slide upper surface were counted on each slide (Figure 2). The chemical−physical water parameters were: T = 20 ± 1 °C; salinity = 30‰; pH = 8.08; photoperiod: 14 h darkness−10 h light; light ∼3000 lx on the top of the boxes.

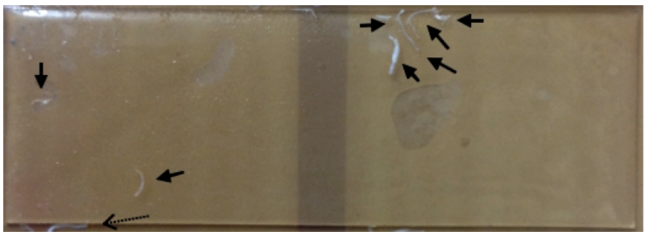

Figure 2. Tube-formed worms (calcareous tube) attached on S100 polymer films; arrows point to eight tubes on the slide; the dotted arrow points to a tube attached on the side edge of the slide (not considered).

2.7.4. Settlement of F. enigmaticus ("No-Choice" Experiment). The method was the same as in ref 26 with slight modifications. Briefly, larvae were collected by filtration (30 μm nylon mesh) and kept at 4 °C for at least 2 h to slow larval movement. Then the selected coatings and glass slides (both not biofilmed) were put in Quadriperm dishes (six replicates per surface). Twenty larvae were pipetted in 1 mL drops of FNSW on each surface. All dishes were then maintained in darkness, at 21 ± 2 °C, covered by wet paper towels to prevent evaporation. Settled larvae were counted at 24 and 48 h.

For both types of experiments, analysis of variance was performed by Kruskal−Wallis' nonparametric test followed by Dunn's multiple comparison test (magnitude values with p < 0.05 were considered statistically significant).

2.7.5. F. enigmaticus Removal Assay. For the removal assay, slides from the "choice" experiment were submitted to a 28 Pa wall shear stress for 5 min. After shear stress, still adhered tubes were counted. Analysis of variance was performed by one-way ANOVA, and means were compared by Dunnet's multiple comparison tests (magnitude values with p < 0.05 were considered statistically significant).

2.7.6. N. salinicola Removal Assay. Briefly, four flasks with a *N. salinicola* culture (in sterile f/2 medium) in logarithmic growth stage were gently rinsed twice with NFSW (S = 35‰). Then a small volume of NFSW (10−20 mL) was put in each flask, and the algal biofilm was resuspended by scraping the flask bottom with a soft sponge. The concentrated suspensions of each flask were mixed and filtered twice (mesh size = 30 μm) to break cell clumps and obtain a most single-cell concentrated suspension. This was then diluted with NFSW. Coatings were put in Quadriperm dishes, and 10 mL of *N. salinicola* diluted suspension (10^6 cells mL^{-1}) was added in each well. Dishes were covered with lids and left on the bench for 2 h.[36] All coatings were then gently rinsed in NFSW to remove unattached cells. Three of the replicates were fixed with 2.5% glutaraldehyde in FSW for 2 h and used for adhesion measurements. After 2 h of fixing, the slides were rinsed three times in deionized water, at least 10 min each time, and then they were left to dry. The other three replicates were used in the detachment assay with the TFCA. Briefly, samples were submitted to a 28 Pa shear stress for 5 min, then they were fixed as described above. Once all samples were fixed, the cells on each slide were counted by

DOI: 10.1021/acsami.5b01522
ACS Appl. Mater. Interfaces 2015, 7, 8293−8301

using an optical microscope (Olympus CH2) equipped with a digital camera (PBI Photo-Bio). Cells were counted on 30 random fields on each slide to calculate percentage detachment.

ANOVA analysis of variance, followed by a Dunnett's test for control comparison (control = PDMS), was adopted to evaluate differences from the control. Magnitude values with $p < 0.05$ were considered statistically significant.

3. RESULTS AND DISCUSSION

3.1. Synthesis. Photo-cross-linked films of a PDMS matrix with methacrylate side chain functionalities were prepared by UV photoinitiated free-radical polymerization in the presence of 1 wt % HMPP photoinitiator. The polyfunctional macromonomer S was alternatively photopolymerized with the polyoxyethylene P3 and fluorinated F monomers to obtain two-component films S*x*P3 and S*x*F, respectively. Moreover, three-component films S*x*P3F*m*/*n* were also prepared by photo-cross-linking of mixtures containing S, P3, and F (Figure 3). Because of the partial miscibility of S and F with P3, it was necessary to add ethyl acetate (~20 wt %) to obtain clear homogeneous mixtures. Mixtures consisting of 1.5−50 wt % P3 or F in the monomer mixture formulation were investigated. However, films S*x*P3 containing more than 10 wt % P3 appeared opaque and rough. On the other hand, although all films containing F were clear and smooth, they were fragile and difficult to handle without breaking when the F content was > 10 wt %. For these reasons, only optically transparent and flexible films having P3 and F ≤ 10 wt % were studied in detail.

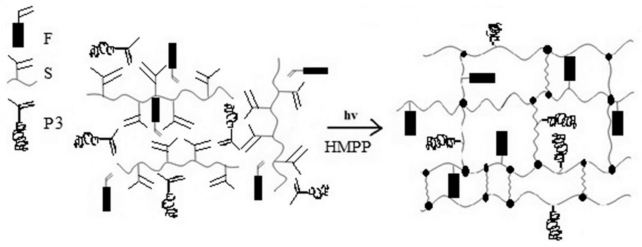

Figure 3. Schematic of the UV photo-cross-linking of a three-component mixture of the methacrylate matrix S with methacrylate P3 and acrylate F monomers.

The progress of photopolymerization was monitored by Fourier transform infrared (FT-IR) spectroscopy, as illustrated in Figure 4 for S100. The absorbance signal at 1639 cm^{-1}, due to the C═C stretching vibration of the methacrylate groups, progressively weakened with UV irradiation time and practically disappeared after 20 min. Spectra recorded at longer irradiation times remained basically unchanged and showed a minor decrease in the absorption intensity between 1660 and 1520 cm^{-1} (Figure 4). Thus, a complete polymerization of the methacrylate functionalities was achieved. Similar results were also obtained in photo-cross-linking the two- and three-component monomer mixtures after 20 min exposures, at which time the monomers P3 and F were fully incorporated into a polymer network structure with their freely moving side chains.

For photo-cross-linking of films for biological tests, the UV irradiation time was 30 min to ensure complete polymerization. Films were obtained by casting the monomer mixtures on Teflon molds or glass slides. After the photocuring, films were dried at room temperature for 24 h and annealed at 120 °C overnight to facilitate the migration of the fluorinated side chains to the surface.

To avoid film delamination, glass slides had previously been functionalized with MAPTS (Figure 5). The surface-tethered methacrylate moieties of MAPTS covalently reacted with the (meth)acrylate groups of the monomer mixture when exposed to UV irradiation and accordingly were also incorporated into the network structure. The polymer film was thereby firmly anchored to the glass surface for subsequent tests.

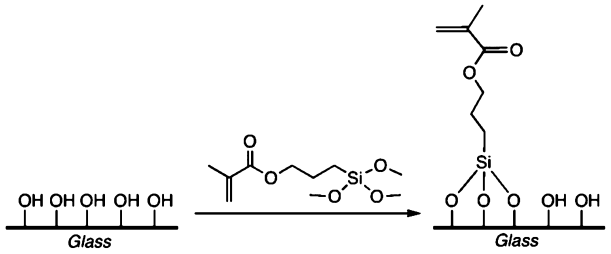

Figure 5. Schematic of glass surface functionalization by MAPTS.

3.2. Swelling. Water uptake and swelling degree of the films were determined to evaluate their stability and resistance to prolonged contact with water in view of their final use in biological assays. As shown in Table 1, the swelling degree gradually increased for all the test samples with increased immersion time in water from 24 to 480 h. Values of the swelling degree obtained after 480-h immersion were higher for films containing the P3 units, being maximal for S90P3 (1.9%).

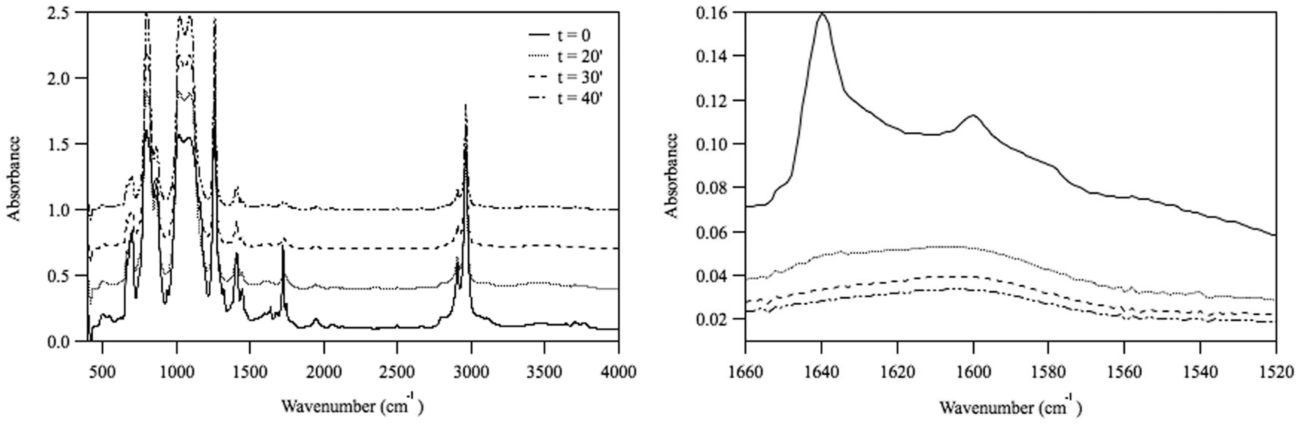

Figure 4. FT-IR spectra recorded for S100 at different times of UV irradiation (left) with the expanded 1660−1520 cm^{-1} region (right).

DOI: 10.1021/acsami.5b01522
ACS Appl. Mater. Interfaces 2015, 7, 8293−8301

Table 1. Swelling Degree of Films at Different Water Immersion Times

	swelling degree[a] (wt %)			
film	24 h	48 h	72 h	480 h
S100	0.1 ± 0.0	0.1 ± 0.0	0.2 ± 0.1	0.4 ± 0.1
S90F	0.3 ± 0.1	0.5 ± 0.2	0.6 ± 0.2	0.6 ± 0.2
S90P3F5/5	0.1 ± 0.1	0.2 ± 0.1	0.3 ± 0.1	1.4 ± 0.3
S90P3	0.3 ± 0.1	0.3 ± 0.2	0.4 ± 0.4	1.9 ± 0.2

[a]Calculated by eq 1.

In any case, the swelling remained very low even after 20 days of water immersion, which indicates that films were resistant to the aquatic environment. Moreover, there was no evidence of chemicals in the extraction waters, and leaching did not occur to a sizable extent (see also ecotoxicological study below).

3.3. Thermal and Dynamic-Mechanical Behavior. Thermal analysis by DSC revealed a glass transition temperature of the polysiloxane matrix at about −125 °C for all films. Moreover, another T_g at about −55 °C appeared clearly evident in the films with a P3 content higher than 2.5 wt % due to the polyoxyethylene dangling chains.

Figure 6 reports the DMTA storage modulus E', loss modulus E'', and loss factor tan δ as a function of temperature for S100 and S90P3F5/5 films. At low temperatures, the elastic modulus was quite high but decreased as the temperature increased with definite drops in correspondence to the main relaxations. However, a prevailing solid-like behavior ($E' > E''$) was observed over the entire temperature region up to 150 °C, which thus suggests a relatively high cross-linking degree. Two relaxation processes were observed for each sample. For S100, a high-intensity peak was detected in the tan δ curve around −130 °C, corresponding to the T_g of polysiloxane matrix. In addition, a low-intensity peak was detected at about −50 °C (Figure 6 left). The storage modulus E' decreased by almost one order of magnitude at the first relaxation and reached a plateau value of 2 MPa at room temperature. The presence of two relaxations suggests the existence of distinct regions differing in their mobility. The lower temperature process corresponds to the glass transition of the polysiloxane chain segments far away from the cross-linking sites, whereas the higher temperature process corresponds to the glass transition of the polysiloxane chain segments close to the cross-linking sites. It is also noteworthy that macromonomer S is characterized by a wide molar mass dispersity possibly accompanied by an uneven distribution of the reactive groups along the polyfunctional polysiloxane chains differing in their lengths. Regions featuring different cross-linking densities and chain flexibility could be ultimately formed during the photo-cross-linking reaction.

The DMTA profile of sample S90P3F5/5 was qualitatively similar to that of S100 with two relaxations at about −130 and −25 °C (Figure 6, right). However, the latter relaxation extended over a wide temperature range between −50 and 20 °C and was structured into several components. Therefore, many factors contributed to this relaxation, including the molar mass and structure heterogeneities, as discussed for S100 as well as the presence of P3 counits leading to a microphase separation between the polysiloxane and polyoxyethylene components, in agreement with the DSC analysis. E' reached a plateau value of 5 MPa at 25 °C.

3.4. Contact Angles and Surface Tension. The contact angles θ for the two- and three-component films were measured with both polar and nonpolar liquids (Table 2). The polysiloxane matrix S100 showed a hydrophobic (θ_w = 103° ± 1°) and lipophilic (θ_h = 32° ± 1°) behavior, in agreement with the wettability of other polysiloxane films.[37,38] The contact angle with isopropanol was very low (θ_{ip} = 16° ± 2°) as a result of the high affinity between polysiloxanes and the test liquid.

The θ_w values of two- and three-component films were generally higher than 100° and not influenced by the presence of P3 or F in the mixture formulations. Although neither θ_h nor θ_{ip} significantly changed with the composition of the three-component films, they seemed to be especially sensitive to the fluorine content in the S*x*F films (e.g., θ_h passed from 32° for S100 to 48° for S95F up to 81° for S90F). *n*-Hexadecane is in fact more sensitive to a fluorine-rich surface, which is hydrophobic and lipophobic,[39] whereas isopropanol is able to better discriminate a silicon-rich surface, which is hydrophobic but not lipophobic.[12]

The films exhibited relatively low surface energy, the γ_S being in the range of 15−24 mN m^{-1} (Table 2). Most of the test films displayed γ_S values very similar to that of the polysiloxane matrix S100, independent of the chemical composition of the mixture. Only S95F and S90F exhibited significantly lower surface tensions as a consequence of the preferential segregation of the fluorinated counits at the polymer−air interface. In the case of three-component films, the surface segregation of the fluorinated chains seemed to be less effective, even for those films containing the same amount as that in the S*x*F films. The tendency of the fluorinated chains to decrease

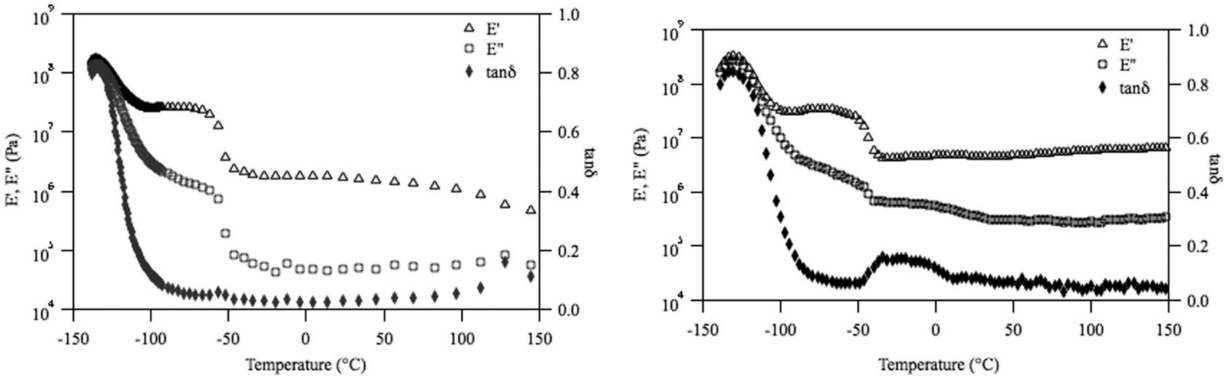

Figure 6. DMTA curves of the moduli E' and E'' and the loss factor tan δ for S100 (left) and S90P3F5/5 (right).

DOI: 10.1021/acsami.5b01522
ACS Appl. Mater. Interfaces 2015, 7, 8293−8301

Table 2. Contact Angles[a] and Surface Tensions[b] of Films before and after 14-Day Immersion in Water

	θ_{ip} (deg)	θ_w (deg)		θ_h (deg)		γ_S (mN m^{-1})	
film	before	before	after	before	after	before	after
S100	16 ± 2	103 ± 1	102 ± 1	32 ± 1	24 ± 3	24.2 ± 0.5	25.8 ± 0.9
S95P3	19 ± 1	102 ± 1	106 ± 2	34 ± 1	32 ± 1	23.9 ± 0.5	23.8 ± 0.6
S90P3	n.d.[c]	104 ± 2	103 ± 2	31 ± 1	27 ± 2	24.3 ± 0.6	25.2 ± 0.8
S95F	24 ± 3	100 ± 2	105 ± 3	48 ± 1	49 ± 2	21.0 ± 1.0	19.8 ± 1.4
S90F	42 ± 2	97 ± 6	99 ± 4	81 ± 4	57 ± 1	15.4 ± 4.4	19.2 ± 2.0
S95P3F5/5	18 ± 2	101 ± 5	105 ± 1	32 ± 3	32 ± 4	24.5 ± 2.0	23.9 ± 1.4
S95P3F3/7	21 ± 1	105 ± 1	105 ± 1	33 ± 1	37 ± 3	23.7 ± 0.5	22.8 ± 1.1
S90P3F7/3	19 ± 1	105 ± 1	103 ± 1	33 ± 3	32 ± 1	23.7 ± 1.1	24.2 ± 0.5
S90P3F5/5	18 ± 1	103 ± 2	103 ± 1	39 ± 2	37 ± 3	22.6 ± 1.1	23.1 ± 1.2

[a]Measured with isopropanol, water, and *n*-hexadecane. [b]Calculated with the Owens−Wendt−Kaelble method. [c]Not determined, decreasing with time.

Table 3. XPS Atomic Composition of the Films before and after 7-Day Water Immersion

		before				after			
film	ϕ (deg)	C (%)	O (%)	Si (%)	F (%)	C (%)	O (%)	Si (%)	F (%)
S95P3F3/7	70	43	13	5	39	56	4	25	15
	20	46	26	19	9	46	23	15	16
	theor.[a]	50	24	24	2				
S95P3F5/5	70	52	27	21	0				
	20	52	27	21	0				
	theor.[a]	50	25	24	1				
S90P3F5/5	70	54	26	20	0	50	26	21	3
	20	53	27	20	0	51	27	21	1
	theor.[a]	51	24	22	3				
S95F	70	58	26	9	7	47	32	14	7
	20	45	21	14	20	33	44	20	3
	theor.[a]	49	24	24	3				
S90F	70	43	15	7	35	49	25	17	9
	20	43	19	11	27	51	27	21	1
	theor.[a]	49	23	22	6				

[a]Atomic percentage calculated on the basis of the nominal composition of the film.

the surface tension was partly compensated by the presence of the polyoxyethylene chains.

With the aim of monitoring contact angles as a function of exposure to water, the films were kept immersed in water for 14 days, and contact angles were then measured with water and *n*-hexadecane (Table 2). Both θ_w and θ_h remained essentially unaffected during 14 days of contact with water for all the films, except S90F, which showed a significant decrease in θ_h. As a consequence, γ_S did not change with immersion in water, except for S90F, for which it increased from 15.5 to 19.2 mN m^{-1}. However, amphiphilic films containing P3 did not increase their hydrophilicity after prolonged exposure to water.

3.5. Surface Chemical Composition. An angle-resolved XPS analysis was performed at two photoemission angles ϕ of 70° and 20° on selected fluorinated films, namely including those to be submitted to biological assays. Experimental data of atomic composition are summarized in Table 3. Both S95F and S90F presented an experimental percentage of fluorine (F_{exp}) higher than the theoretical one (F_{theor}) calculated on the basis of the nominal composition of the film (e.g., F_{exp} = 35% at ϕ = 70° and F_{theor} = 6% for S90F). Such surface enrichment in fluorine resulted in a significant depletion in silicon content (e.g., Si_{exp} = 7% at ϕ = 70° and Si_{theor} = 22% for S90F). Accordingly, the fluorinated chains were preferentially segregated at the polymer−air interface, driven by their lowest surface tension. The F_{exp}/F_{theor} ratio at ϕ = 70° almost tripled by doubling the nominal amount of F in the two-component films. Moreover, while for S90F, the F atomic percentage decreased with ϕ, that is, with increasing sampling depth, for S95F, it followed the opposite trend and passed from 7% at ϕ = 70° to 20% at ϕ = 20°. This shows that the surface segregation of the perfluorohexyl chains was less effective in the film containing the lower amount of fluorinated counits because of restrained mobility across the cross-linked matrix.

A peculiar behavior was observed for the films derived from the three-component mixtures. In fact, two of the three test films (S95P3F5/5 and S90P3F5/5) did not display fluorine at any photoemission angle (Table 3). By contrast, F_{exp} for S95P3F3/7 was much higher than F_{theor} (2%) and markedly decreased with the sampling depth, passing from 39% (ϕ = 70°) to 9% (ϕ = 20°). The sample S95P3F3/7 had an intermediate fluorine atomic percentage but the lowest content of P3 chains with respect to the other three-component blends. Therefore, at this higher P3/F ratio, the chemical structure of the polymer network is modified so as to prevent the migration of the perfluoroalkyl chains. This is in agreement with the above results of contact angle measurements.

Those films that had exhibited fluorine at the surface in the dry state were also investigated by angle-resolved XPS after being immersed in water for 7 days (Table 3). The elemental analysis showed a large decrease in fluorine and increase in silicon contents after immersion in water for the films of S90F

DOI: 10.1021/acsami.5b01522
ACS Appl. Mater. Interfaces 2015, 7, 8293−8301

and S95P3F3/7 with a high F_{exp}/F_{theor} ratio (~6 and ~19, respectively) in the dry state. These results clearly point to a surface reconstruction. This seems to involve the moving of the fluorinated chains away from the surface rather than the migration of the polyoxyethylene chains to come in contact with water, even at the relatively high P3/F ratio. Consistently, S95F having 7% fluorine at ϕ = 70° did not undergo a significant surface reconstruction, as the driving force of the fluoroalkyl chains to hide themselves in the inner molecular layers was limited by the low fluorine content at the outer surface of the films in the dry state.

3.6. Biological Tests. Two- and three-component films with a high content of S (90–95 wt %) were chosen for testing against *F. enigmaticus* and *N. salinicola* to assess whether the low amount of P3 or F chains would be sufficient to affect their AF/FR performance. Prior to biological assays, an ecotoxicological study was performed on the leachates of the films using the bacterium *Vibrio fischeri*, the unicellular alga *Dunaliella tertiolecta*, and the crustacean *Artemia franciscana* as testing organisms[30] (see Supporting Information). The water leachates of the films showed no acute nor chronic toxicity against any of the three species.

3.6.1. Settlement of F. enigmaticus ("Choice" and "No-Choice" Experiments). The assays for the evaluation of AF performance started from available information on different "no-choice" and "choice" experiments with *F. enigmaticus* and other serpulids.[26,35]

Following a "no-choice" method,[26] the adhesion of competent larvae was "forced" by directly pipetting the organisms on the test surfaces (without biofilm). After 48 h, competent larvae with a partially formed proteinaceous tube and modified prototroch settled with percentage values of 15.0 ± 2.5 and 13.3 ± 3.1 for glass and S100, respectively. These results are comparable to those reported for glass and PDMS (10.2 and 11.1%, respectively).[26] For all other surfaces, total absence of adhesion was observed.

Following a "choice" method,[35] a large number of free swimming larvae was left "free" to adhere on randomly submerged slides (with a 10-day natural biofilm). Therefore, the rationale of this kind of settlement assay was based on the tendency of swimming larvae to adhere on a vertical surface. Initial experiments performed on horizontally/vertically placed glass slides had shown that the free swimming larvae solely settled on vertically placed surfaces with a zero percentage adhesion on horizontally oriented surfaces (data not shown). The surfaces were biofilmed to homogenize larval-attracting surface cues to prevent any initial bias for a particular surface. This was not necessary for the "no-choice" experiment. The biofilms were homogeneous and covered uniformly the whole test surfaces without patches at macroscopic/microscopic observations (Figure S4, Supporting Information). Different percentages of adhesion were observed on all tested surfaces (Figure 7): maximum number of 2–4 mm adhered calcified tubes was 16.7 ± 4.5 on glass, while mean number of adhered calcified tubes on polymer films ranged from 3.7 ± 1.2 (S95P3F5/7) to 8.0 ± 1.4 (S95P3). The settlement of *F. enigmaticus* on glass was significantly different from S95P3F5/5 and S95P3 films (Dunn's test, $p \leq 0.001$). Although settlement was lower on two- and three-component films richer in P3 compared to those richer in F, this difference was not significant.

3.6.2. F. enigmaticus Removal Assay. For the removal assay, 18-day worms with well-formed calcified tubes (2–4 mm length) were used in the TCFA test. The removal percentage of *F. enigmaticus* after exposure to a wall shear stress of 28 Pa in the flow channel is shown in Figure 8. Tubeworms were attached much less strongly to S95P3 and S95P3F5/5, which performed (100% detachment) as well as the glass standard. On the other hand, films containing more than 2.5 wt % F showed lower release of *F. enigmaticus* (S90F: 64.0% detachment), which did not significantly differ from that of the S100 control (60.8% detachment). Thus, chemical composition of the polymer films markedly affected their FR properties with an ascending trend of removal percentage with the content of P3 in the film, with complete removal seemingly being achieved at ~2.5 wt % P3. The fluorinated S95P3F5/5 film showed a removal percentage as high as that of S95P3, not containing fluorine. However, XPS results (see above) highlighted the absence of fluorine in the outermost surface layers of the S95P3F5/5 film despite the 2.5 wt % fluorine nominal content. The two films exhibited similar chemical surface composition, which resulted in similar maximal FR properties. Other serpulids such as *Hydroides dianthus* and *Hydroides elegans* have been used in tube-removal experiments.[40,41] Zardus et al. performed experiments on the removal of primary and secondary tubes of *H. elegans* from a glass substrate in a TCFA similar to that used in this study.[35] Namely, they used 2 h-proteinaceous primary tubes and 12 h-calcified secondary tubes and showed that a wall shear stress of 50 Pa was just enough to remove a small percentage of adhered secondary tubes from a biofilmed glass. By contrast, a shear stress of 28 Pa

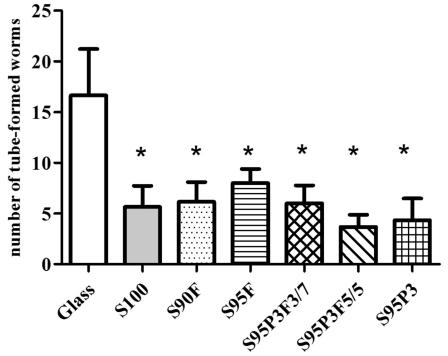

Figure 7. Number (mean ± SD) of 2–4 mm adhered calcified tubes. *, Significantly different from glass ($p \leq 0.001$, Kruskal–Wallis' nonparametric test, Dunn's test).

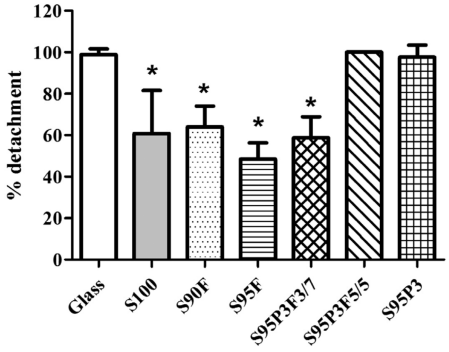

Figure 8. Percent detachment (mean ± SD) of calcified tube-formed worms after a 28 Pa wall shear stress. *, Significantly different from glass ($p \leq 0.001$, one-way ANOVA, Dunnet's test).

DOI: 10.1021/acsami.5b01522
ACS Appl. Mater. Interfaces 2015, 7, 8293–8301

was here sufficient to remove from 40% up to 100% of worms from any tested surfaces.

3.6.3. N. salinicola Removal Assay. The results obtained with *N. salinicola* were comparable with literature findings (Figure 9).[36,42] A shear stress of 28 Pa was sufficient to remove

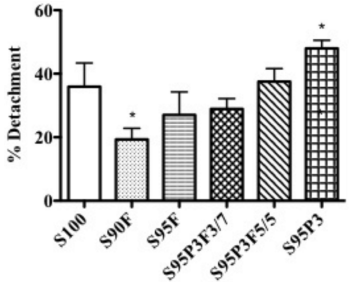

Figure 9. Percent removal (mean ± SD) of *N. salinicola* at 28 Pa shear stress. *, Significantly different from S100 control ($p \leq 0.001$, one-way ANOVA, Dunnet's test).

35.9 ± 7.4% of adhered cells on S100 films. The film S95P3 showed a significantly higher percentage (47.9 ± 7.4%) of cell removal than the matrix S100. S90F showed the lowest significant cell removal (19.3 ± 3.5%). The mean of removed cells of the other coatings did not significantly differ from S100 matrix. Thus, incorporation of hydrophilic polyoxyethylene units into the PDMS matrix favors an enhanced removal of the diatom *N. salinicola*. These results are consistent with previous findings on removal tests of the diatom *N. perminuta* from SEBS-matrix coatings containing polyoxyethylene and polysiloxane chain units.[43] By contrast, *N. perminuta* is reported to strongly adhere to highly hydrophobic, for example, purely fluorinated, polymer surfaces.[44]

4. CONCLUSIONS

A simple method was introduced to develop new practical PDMS-based films for AF/FR application. Two- and three-component films were prepared by photopolymerizing a polysiloxane macromonomer S carrying methacrylate side groups with polyoxyethylene P3 or fluorinated F monomers without resorting to conventional heavy-metal catalyzed cross-linking reactions. Neither the low elastic modulus nor the low surface tension of the films depended significantly on the coating formulation in the investigated range, whereas the chemical composition of the film surface and its reconstruction after contact with water were markedly affected by the P3/F ratio.

The films were tested against the serpulid *F. enigmaticus*, a new and significant marine biofoulant. The FR properties were markedly influenced by the film formulation. Both *N. salinicola* and *F. enigmaticus* were easily removed from films richer in polyoxyethylene units, with highest removal being detected for films with a P3 content as low as 2.5 wt %. By contrast, the tested organisms adhered strongly to surfaces enriched in fluorine. Other widespread foulants are known to have contrasting tendencies to adhere to hydrophilic/hydrophobic surfaces.[16,45] Ongoing investigations aim to better ascertain what role the hydrophilic/hydrophobic, that is, amphiphilic, nature of the polymer film surface may play in effecting the biological performance against *F. enigmaticus*. This biofoulant is resistant to salinity fluctuations and could also be suitably used for AF/FR studies in brackish water ecosystems.

■ ASSOCIATED CONTENT

Supporting Information

Ecotoxicological assays with *V. fischeri*, *D. tertiolecta*, and *A. franciscana*; calibration of turbulent channel flow apparatus; biofilmed surfaces for assay with *F. enigmaticus*. This material is available free of charge via the Internet at http://pubs.acs.org.

■ AUTHOR INFORMATION

Corresponding Author

*E-mail: giancarlo.galli@unipi.it.

Notes

The authors declare no competing financial interest.

■ ACKNOWLEDGMENTS

This work was supported by the EC Framework 7 "SEACOAT" project and the Italian MiUR (PRIN fondi 2010-2011). The authors also thank Dr. A. Glisenti (University of Padova) for assistance with the XPS experiments.

■ REFERENCES

(1) Omae, I. Organotin Antifouling Paints and Their Alternatives. *Appl. Organomet. Chem.* **2003**, *17*, 81−105.
(2) Yebra, D. M.; Kiil, S.; Dam-Johansen, K. Antifouling Technology—Past, Present, and Future Steps Towards Efficient and Environmentally Friendly Antifouling Coatings. *Prog. Org. Coat.* **2004**, *50*, 75−104.
(3) Sonak, S.; Pangam, P.; Giriyan, A.; Hawaldar, K. J. Implications of the Ban on Organotins for Protection of Global Coastal and Marine Ecology. *Environ. Manage.* **2009**, *90*, S96−S108.
(4) Thomas, K. V.; Brooks, S. The Environmental Fate and Effects of Antifouling Paint Biocides. *Biofouling* **2010**, *26*, 73−88.
(5) Lejars, M.; Margaillan, A.; Bressy, C. Fouling Release Coatings: A Nontoxic Alternative to Biocidal Antifouling Coatings. *Chem. Rev.* **2012**, *112*, 4347−4390.
(6) Callow, J. A.; Callow, M. E. Trends in the Development of Environmentally Friendly Fouling-Resistant Marine Coatings. *Nature Commun.* **2011**, *2*, 244.
(7) Gudipati, C. S.; Finlay, J. A.; Callow, J. A.; Callow, M. E.; Wooley, K. L. The Antifouling and Fouling-Release Performance of Hyperbranched Fluoropolymer (HBFP)-Poly(ethylene glycol) (PEG) Composite Coatings Evaluated by Adsorption of Biomacromolecules and the Green Fouling Alga *Ulva*. *Langmuir* **2005**, *21*, 3044−3053.
(8) Imbesi, P. M.; Gohad, N. V.; Eller, M. J.; Orihuela, B.; Rittschof, D.; Schweikert, E. A.; Mount, A. S.; Wooley, K. L. Noradrenaline-Functionalized Hyperbranched Fluoropolymer-Poly(ethylene glycol) Cross-linked Networks as Dual-Mode, Anti-Biofouling Coatings. *ACS Nano* **2012**, *6*, 1503−1512.
(9) Krishnan, S.; Ayothi, R.; Hexemer, A.; Finlay, J. A.; Sohn, K. E.; Perry, R.; Ober, C. K.; Kramer, E. J.; Callow, M. E.; Callow, J. A. Anti-Biofouling Properties of Comb-like Block Copolymer with Amphiphilic Side Chains. *Langmuir* **2006**, *22*, 5075−5086.
(10) Weinman, C. J.; Finlay, J. A.; Park, D.; Paik, M. Y.; Krishnan, S.; Sundaram, H. S.; Dimitriou, M.; Sohn, K. E.; Callow, M. E.; Callow, J. A. ABC Triblock Surface Active Block Copolymer with Grafted Ethoxylated Fluoroalkyl Amphiphilic Side Chains for Marine Antifouling/Fouling-Release Applications. *Langmuir* **2009**, *25*, 12266−12274.
(11) Martinelli, E.; Suffredini, M.; Galli, G.; Glisenti, A.; Pettitt, M. E.; Callow, M. E.; Callow, J. A.; Williams, D.; Lyall, G. Amphiphilic Block Copolymer/Poly(dimethylsiloxane) (PDMS) Blends and Nanocomposites for Improved Fouling-Release. *Biofouling* **2011**, *27*, 529−541.
(12) Martinelli, E.; Sarvothaman, M. K.; Alderighi, M.; Galli, G.; Mielczarski, E.; Mielczarski, J. A. PDMS Network Blends of Amphiphilic Acrylic Copolymers with Poly(ethylene glycol)-Fluoroalkyl Side Chains for Fouling-Release Coatings. I. Chemistry and

DOI: 10.1021/acsami.5b01522
ACS Appl. Mater. Interfaces 2015, 7, 8293−8301

Stability of the Film Surface. *J. Polym. Sci., Part A: Polym. Chem.* **2012**, *50*, 2677−2686.
(13) Sommer, S.; Ekin, A.; Webster, D. C.; Stafslien, S.; Daniels, J.; Van der Wal, L. J.; Thompson, S. E. Y.; Callow, M. E.; Callow, J. A. A Preliminary Study on the Properties and Fouling-Release Performance of Siloxane−Polyurethane Coatings Prepared from Poly(dimethylsiloxane) (PDMS) Macromers. *Biofouling* **2010**, *26*, 961−972.
(14) Wang, Y.; Pitet, L. M.; Finlay, J. A.; Brewer, L. H.; Cone, G.; Betts, D. E.; Callow, M. E.; Callow, J. A.; Wendt, D. E.; Hillmyer, M. A.; De Simone, J. M. Investigation of the Role of Hydrophilic Chain Length in Amphiphilic Perfluoropolyether/Poly(ethylene glycol) Networks: Towards High Performance Antifouling Coatings. *Biofouling* **2011**, *27*, 1139−1150.
(15) Wang, Y.; Finlay, J. A.; Betts, D. E.; Merkel, T. J.; Luft, J. C.; Callow, M. E.; Callow, J. A.; De Simone, J. M. Amphiphilic Conetworks with Moisture-Induced Surface Segregation for High-Performance Nonfouling Coatings. *Langmuir* **2011**, *27*, 10365−10369.
(16) Martinelli, E.; Sarvothaman, M. K.; Galli, G.; Pettitt, M. E.; Callow, M. E.; Callow, J. A.; Conlan, S. L.; Clare, S. A.; Sugiharto, A. B.; Davies, C.; Williams, D. Poly(dimethyl siloxane) (PDMS) Network Blends of Amphiphilic Acrylic Copolymers with Poly(ethylene glycol)-Fluoroalkyl Side Chains for Fouling-Release Coatings. II. Laboratory Assays and Field Immersion Trials. *Biofouling* **2012**, *28*, 571−582.
(17) (a) Cui, J.; Lackey, M. A.; Tew, G. N.; Crosby, A. J. Mechanical Properties of End-Linked PEG/PDMS Hydrogels. *Macromolecules* **2012**, *45*, 6104−6110. (b) Hou, Y.; Schoener, C. A.; Regan, K. R.; Munoz-Pinto, D.; Hahn, M. S.; Grunlan, M. A. Photo-Cross-Linked PDMSstar-PEG Hydrogels: Synthesis, Characterization, and Potential Application for Tissue Engineering Scaffolds. *Biomacromolecules* **2010**, *11*, 648−656.
(18) Aldred, N.; Clare, A. S. The Adhesive Strategies of Cyprids and Development of Barnacle-Resistent Marine Coatings. *Biofouling* **2008**, *24*, 351−363.
(19) Briand, J. F. Marine Antifouling Laboratory Bioassays: An Overview of Their Diversity. *Biofouling* **2009**, *25*, 297−311.
(20) Mieszkin, S.; Martin-Tanchereau, P.; Callow, M. E.; Callow, J. A. Effect of Bacterial Biofilms Formed on Fouling-Release Coatings from Natural Seawater and *Cobetia marina* on the Adhesion of Two Marine Algae. *Biofouling* **2012**, *28*, 953−968.
(21) Sokolova, A.; Cilz, N.; Daniels, J.; Stafslien, S. J.; Brewer, L. H.; Wendt, D. E.; Bright, F. V.; Detty, M. R. A Comparison of the Antifouling/Foul-Release Characteristics of Nonbiocidal Xerogel and Commercial Coatings Toward Micro- and Macrofouling Organisms. *Biofouling* **2012**, *28*, 511−523.
(22) Fauvel, P. Un Nouveau Serpulien d'Eau Saumâtre, *Merceriella* n.g., *enigmatica* n.sp. *Bull. Soc. Zool Fr.* **1923**, *47*, 424−430.
(23) Straughan, D. Ecological Studies of *Mercierella enigmatica Fauvel* (*Annelida: Polychaeta*) in the Brisbane River. *J. Anim. Ecol.* **1972**, *41*, 93−136.
(24) Eno, N. C.; Clark, R. A.; Sanderson W. G. *Non-native Marine Species in British Waters: A Review and Directory*; Joint Nature Conservation Committee: Peterborough, UK, 1997; p 152.
(25) Hove, H. A.; Kupriyanova, E. K. Taxonomy of *Serpulidae* (*Annelida*, *Polychaeta*): The State of Affairs. *Zootaxa* **2009**, *2036*, 121−126.
(26) Gabilondo, R.; Graham, H.; Caldwell, G. S.; Clare, A. S. Laboratory Culture and Evaluation of the Tubeworm *Ficopomatus enigmaticus* for Biofouling Studies. *Biofouling* **2013**, *29*, 869−878.
(27) Owens, D. K.; Wendt, R. C. Estimation of the Surface Free Energy of the Polymers. *J. Appl. Polym. Sci.* **1969**, *13*, 1741−1747.
(28) Kaelble, D. H. Dispersion-Polar Surface Tension Properties of Organic Solids. *J. Adhes.* **1970**, *2*, 66−81.
(29) Shirley, D. A. High-Resolution X-ray Photoemission Spectrum of the Valence Bands of Gold. *Phys. Rev. B* **1972**, *5*, 4709−4714.
(30) Pretti, C.; Oliva, M.; Mennillo, E.; Barbaglia, M.; Funel, M.; Yasani, B. R.; Martinelli, E.; Galli, G. An Ecotoxicological Study on Tin- and Bismuth-Catalysed PDMS Based Coatings Containing a Surface-Active Polymer. *Ecotoxicol. Environ. Saf.* **2013**, *98*, 250−256.
(31) Hussain, A. K. M. F.; Reynolds, W. C. Measurements in Fully Developed Turbulent Channel Flow. *J. Fluids Eng.* **1975**, *97*, 568−578.
(32) Hadfield, M. G.; Unabia, C. C.; Smith, C. M.; Michael, T. M. Settlement Preferences of the Ubiquitous Fouler *Hydroides elegans*. *Recent Developments in Biofouling Control*; Fingerman, M., Nagabhushanam, R., Sarojin, R., Eds.; Oxford and IBH: New Delhi, 1994; pp 65−74.
(33) Nedved, B. T.; Hadfield, M. G. *Hydroides elegans* (*Annelida*: *Polychaeta*): A Model for Biofouling Research. *Marine and Industrial Biofouling. Springer Series on Biofilms*; Flemming, H. C., Venkatesan, R., Murthy, S. P., Cooksey, K., Eds.; Springer-Verlag: Berlin, Germany, 2009; pp 203−217.
(34) Toonen, R. J.; Pawlik, J. R. Settlement of the Tube Worm *Hydroides dianthus* (*Polychaeta: Serpulidae*): Cues for Gregarious Settlement. *Mar. Biol.* **1996**, *126*, 725−733.
(35) Zardus, J. D.; Nedved, B. T.; Huang, Y.; Tran, C.; Hadfield, M. G. Microbial Biofilms Facilitate Adhesion in Biofouling Invertebrates. *Biol. Bull.* **2008**, *214*, 91−98.
(36) Schultz, M. P.; Finlay, J. A.; Callow, M. E.; Callow, J. A. A Turbulent Channel Flow Apparatus for the Determination of the Adhesion Strength of Microfouling Organisms. *Biofouling* **2000**, *15*, 243−251.
(37) Yasani, B. R.; Martinelli, E.; Galli, G.; Glisenti, A.; Mieszkin, S.; Callow, M. E.; Callow, J. A. A Comparison Between Different Fouling-Release Elastomer Coatings Containing Surface-Active Polymers. *Biofouling* **2014**, *30*, 387−399.
(38) Martinelli, E.; Guazzelli, E.; Bartoli, C.; Gazzarri, M.; Chiellini, F.; Galli, G. Amphiphilic Pentablock Copolymers and Their Blends with PDMS for Antibiofouling Coatings. *J. Polym. Sci., Part A: Polym. Chem.* **2015**, *53*, 1213−1225.
(39) Martinelli, E.; Galli, G.; Glisenti, A. Surface Behavior of Modified-Polystyrene Triblock Copolymers with Different Macromolecular Architectures. *Eur. Polym. J.* **2014**, *60*, 69−78.
(40) Kavanagh, C. J.; Schultz, M. P.; Swain, G. W.; Stein, J.; Truby, K.; Wood, C. D. Variation in Adhesion Strength of *Balanus eburneus*, *Crassostrea virginica*, and *Hydroides dianthus* to Fouling-Release Coatings. *Biofouling* **2001**, *17*, 155−167.
(41) Holm, E. R.; Kavanagh, C. J.; Meyer, A. E.; Wiebe, D.; Nedved, B. T.; Wendt, D.; Smith, C. M.; Hadfield, M. G.; Swain, G.; Wood, C. D.; Truby, K.; Stein, J.; Montemarano, J. Interspecific Variation in Patterns of Adhesion of Marine Fouling to Silicone Surfaces. *Biofouling* **2006**, *22*, 233−243.
(42) Zhou, Z.; Calabrese, D. R.; Taylor, W.; Finlay, J. A.; Callow, M. E.; Callow, J. A.; Fischer, D.; Kramer, E. J.; Ober, C. K. Amphiphilic Triblock Copolymers with PEGylated Hydrocarbon Structures as Environmentally Friendly Marine Antifouling and Fouling-Release Coatings. *Biofouling* **2014**, *30*, 589−604.
(43) Sundaram, H. S.; Cho, Y.; Dimitriou, M. D.; Weinman, C. J.; Finlay, J. A.; Cone, G.; Callow, M. E.; Callow, J. A.; Kramer, E. J.; Ober, C. K. Fluorine-Free Mixed Amphiphilic Polymers Based on PDMS and PEG Side Chains for Fouling Release Applications. *Biofouling* **2011**, *27*, 589−602.
(44) Krishnan, S.; Wang, N.; Ober, C. K.; Finlay, J. A.; Callow, M. E.; Callow, J. A.; Hexemer, A.; Sohn, K. E.; Kramer, E. J.; Fischer, D. A. Comparison of the Fouling Release Properties of Hydrophobic Fluorinated and Hydrophilic PEGylated Block Copolymer Surfaces: Attachment Strength of the Diatom *Navicula* and the Green Alga *Ulva*. *Biomacromolecules* **2006**, *7*, 1449−1462.
(45) Finlay, J. A.; Krishnan, S.; Callow, M. E.; Callow, J. A.; Dong, D.; Asgill, N.; Wong, K.; Kramer, E. J.; Ober, C. K. Settlement of *Ulva* Zoospores on Patterned Fluorinated and PEGylated Monolayer Surfaces. *Langmuir* **2008**, *24*, 503−510.

DOI: 10.1021/acsami.5b01522
ACS Appl. Mater. Interfaces 2015, 7, 8293−8301